# Influence of Rigidity and Knot Complexity on the Knotting of Confined Polymers

Peter Poier,* Christos N. Likos, and Richard Matthews

Faculty of Physics, University of Vienna, Boltzmanngasse 5, A-1090 Vienna, Austria

ABSTRACT: We employ computer simulations and thermodynamic integration to analyze the effects of bending rigidity and slit confinement on the free energy cost of tying knots, $\Delta F_{knotting}$, on polymer chains under tension. A tension-dependent, nonzero optimal stiffness κ_{min} exists, for which $\Delta F_{knotting}$ is minimal. For a polymer chain with several stiffness domains, each containing a large amount of monomers, the domain with stiffness κ_{min} will be preferred by the knot. A *local* analysis of the bending in the interior of the knot reveals that local stretching of chains at the braid region is responsible for the fact that the tension-dependent optimal stiffness has a nonzero value. The reduction in $\Delta F_{knotting}$ for a chain with optimal stiffness relative to the flexible chain can be enhanced by tuning the slit width of the 2D confinement and increasing the knot complexity. The optimal stiffness itself is independent of the knot types we considered, while confinement shifts it toward lower values.
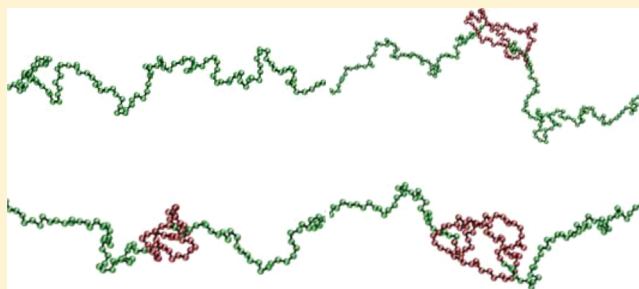
1. INTRODUCTION

While in the macroscopic world it is clear that the effort needed to tie a knot in wire or string will always increase if it is made more rigid, for equivalent microscopic objects, polymers, the same does not hold. Instead, it is found that the free energy cost of knotting a polymer, $\Delta F_{knotting}$, has a minimum at a nonzero stiffness.[1] This finding is particularly interesting in the context of biological macromolecules, such as DNA or RNA, where on the one hand knotting is known to occur[2,3] and has significant effects on key processes,[4−6] while on the other rigidity may depend sensitively on the base sequence,[7−9] leading to varying flexibility along the polymer. Furthermore, there is evidence of correlations between DNA stiffness and sites preferred by type II topoisomerases,[1] enzymes that regulate knotting.[10]

It is expected that the rigidity dependence of $\Delta F_{knotting}$ will affect the behavior of knots in DNA with nonuniform flexibility, for example by localizing them in regions with favorable stiffness. However, previous work[1] neglected a key qualitative feature of biological DNA, namely that it is typically highly confined.[11−13] Confinement of a knotted polymer in a good solvent may significantly affect its properties. For example, in contrast to three dimensions where they are weakly localized, knots in polymers adsorbed on a surface are strongly localized.[14,15] Considering the properties of polymers confined in a slit, simulations of DNA found a nonmonotonic dependence of the knotting probability on the slit width,[16] and for flexible polymers evidence was found that the particular topology is important.[17] While previous work on knotting in confinement has focused on polymers that have one specific stiffness, here we apply a simple model for a polymer chain under tension to investigate the dependence of $\Delta F_{knotting}$ on rigidity for various widths of the geometrical confinement. We

find that a local stretching of the chains at the braiding region of the knots is responsible for the fact that the optimal bending rigidity for knot formation, κ_{min}, differs from zero. Geometric confinement, however, pushes this optimal rigidity toward smaller values. The effect of confinement on κ_{min} as well as the amount by which $\Delta F_{knotting}$ is reduced for the optimal rigidity κ_{min} depends sensitively on the tension applied to the polymer chain.

The rest of the paper is organized as follows: We first present our model and details about the simulation in section 2. In section 3 we define and explain the observables that have been measured in our simulations. In particular, we define our notion of *bending* of the polymer chain and establish its connection to $\Delta F_{knotting}$. Section 4 introduces the analysis of the *local bending* in the interior of the knot, which is carried out to investigate which part of the knot is responsible for the reduction of $\Delta F_{knotting}$ for polymers with nonzero bending stiffness κ_{min} relative to a fully flexible chain. We present our results in section 5, whereas in section 6 we summarize and draw our conclusions.

2. MODEL AND SIMULATION DETAILS

For the polymer chain (linear or knotted), we employ a standard, self-avoiding bead−spring model with rigidity κ, confined parallel to the (x,z)-plane and under tension τ. The interaction part of the Hamiltonian thus reads as

$$V(\{\mathbf{r}_i\}) = \kappa \sum_i (1 - \hat{\mathbf{r}}_{i-1,i} \cdot \hat{\mathbf{r}}_{i,i+1}) - \frac{kR_0^2}{2} \times$$

$$\sum_i \ln\left[1 - \left(\frac{\mathbf{r}_{i,i+1}}{R_0}\right)^2\right] + 4\varepsilon \sum_{j>i} \sum_i \left[\left(\frac{\sigma}{r_{i,j}}\right)^{12} - \left(\frac{\sigma}{r_{i,j}}\right)^6 + \frac{1}{4}\right]$$

$$\times \Theta(2^{1/6}\sigma - r_{i,j}) + k_B T \sum_i \left(\frac{y_i}{d}\right)^2 - \tau L_z \tag{1}$$

In eq 1, $\mathbf{r}_{i,j} = \mathbf{r}_j - \mathbf{r}_i$ is the vector from bead i to bead j, located at position vectors $\mathbf{r}_i$ and $\mathbf{r}_j$, respectively, with the unit vector $\hat{\mathbf{r}}_{i,j} = \mathbf{r}_{i,j}/|\mathbf{r}_{i,j}|$. The first term represents the bending energy of the chain, where κ is the bending rigidity. The second and third terms are the connectivity and steric terms, respectively, whereas $\Theta(\omega)$ is the Heaviside step function of ω, which renders the Lennard-Jones potential purely repulsive. We choose $\varepsilon = k_B T$, $k = 30k_B T/\sigma^2$, and $R_0 = 1.5\sigma$, preventing the chain from crossing itself and thus conserving its topology. The chain is confined in a slit parallel to the (x, z) plane, which is realized via a harmonic external potential acting on the y-component of the coordinate of each monomer, expressed by the fourth term in eq 1. The last term applies a tension τ on the chain along the z-direction of the setup, with L_z denoting the extension of the chain along this direction.

We used the LAMMPS simulation package[18] to carry out constant-$N\tau T$ molecular dynamics (MD) simulations. The polymers consist of $N = 256$ monomers for the chains simulated at tensions $\tau = 0.8\ k_B T/\sigma$ and $\tau = 0.4\ k_B T/\sigma$ and of $N = 512$ monomers for the simulations at tensions $\tau = 0.2\ k_B T/\sigma$ and $\tau = 0.1\ k_B T/\sigma$. The longer polymer chains at the two smaller tensions are necessary due to the larger knot size for these tension values. The chains are placed in a simulation box with volume $V = 100\sigma \times 150\sigma \times L_z$ at the two higher tensions and $V = 200\sigma \times 300\sigma \times L_z$ for the lower tensions. The tension τ is realized via a barostat coupled to the fluctuating z-length of the simulation box, while the box lengths in the x- and y-directions are fixed to 100σ and 150σ for the higher tensions 200σ and 300σ for the lower tensions, respectively. The polymer is connected across the periodic boundary conditions in the z-direction to guarantee that the knot is preserved. We also use periodic boundary conditions in the x-direction, while for the y-direction confinement prevents the polymer chain from getting outside the simulation box. For both the thermostat and the barostat, we used a Nosé–Hoover chain with 3 degrees of freedom.[19] With m denoting the monomer mass and $\beta = (k_B T)^{-1}$, $t_0 = (m\sigma^2\beta)^{1/2}$ sets the unit of time. We integrated the equations of motion with a time step $\Delta t = 10^{-3}t_0$. The equilibration time was 2×10^7 time steps, and data were collected during a total of 3×10^8 time steps.

3. DEFINITION AND INTERPRETATION OF OBSERVABLES

Definition and Physical Interpretation of $\Delta F_{knotting}(\kappa)$.
Let $F_{lin,knot}(\kappa)$ be the free energies of an unknotted and a knotted chain, respectively, for given κ, τ, and chain length. We define $\Delta F_{knotting}(\kappa) \equiv F_{knot}(\kappa) - F_{lin}(\kappa)$, a quantity that gives a measure for the effort to tie a knot into the chain of N monomers. In our simulations, we do not calculate the absolute value for $\Delta F_{knotting}(\kappa)$ but its value relative to $\Delta F_{knotting}(\kappa = 0)$ of a flexible chain, a procedure that removes the N-dependence for a linear and a knotted chain of the same degree of polymerization N. Thus, we calculate $\Psi(\kappa) \equiv \Delta F_{knotting}(\kappa) - \Delta F_{knotting}(0)$, which has a direct physical interpretation: Let us

consider a long polymer chain with various domains, which differ by their respective bending stiffness κ_i and the number of monomers they contain N_i. Then, the quantity $\Psi(\kappa)$ allows us to predict the probability for the knot to be found in the ith domain relative to the probability for it being in the jth domain as

$$\frac{P_i}{P_j} = \frac{N_i}{N_j} \exp[-\beta(\Psi(\kappa_i) - \Psi(\kappa_j))] \tag{2}$$

An implicit assumption entering eq 2 is that the length of chain segments, N_i, is much longer than the knot size N_K, so that for most configurations the part of the polymer chain that is affected by the knot is localized in only one of the domains. Because of the applied tension τ, the knotted part of the chain will always remain finite. In ref 1 it was shown that at fixed κ the size of the knot does not scale with N, the number of monomers on the chain, but rather as $N_K \sim (k_B T/\tau)^\alpha$ with some exponent α. The reason for this is that the stretched polymer forms a series of tension blobs,[20] whose size scales with the tension τ but not with N. The knot can only be in one of those blobs; therefore, N_K will be finite for any nonzero tension τ. Therefore, for sufficiently large N_i, eq 2 indeed provides a good prediction for P_i. In ref 1 the prediction of eq 2 was tested for a simulation of a polymer chain with two stiffness domains.

Definition and Interpretation of the Chain's Bending $\hat{B}$. With $\hat{\mathbf{r}}_{j,j+1}$ denoting the unit vector between monomers j and $j + 1$, we define the quantity

$$\hat{B} \equiv \sum_i (1 - \hat{\mathbf{r}}_{i-1,i} \cdot \hat{\mathbf{r}}_{i,i+1}) \tag{3}$$

for any configuration of its monomers and call it the *bending* of the chain; evidently it holds that $\hat{B} \geq 0$. One can check that this definition of the bending is sensible for various special cases. For instance, for a configuration with a straight polymer chain this definition gives the minimum value for $\hat{B}$, namely $\hat{B} = 0$. The contribution to $V(\{\mathbf{r}_i\})$ defined in (1) due to the bending stiffness is $\kappa\hat{B}$. Moreover $B_T(\kappa) \equiv \langle\hat{B}\rangle$ is the thermodynamic expectation value of the same for a chain of topology $T \in \{\text{knot, linear}\}$.

With $F_T(\kappa)$ denoting the free energy of the polymer, it holds that $\partial F_T(\kappa)/\partial\kappa = B_T(\kappa)$. This allows us to calculate how the cost of knotting changes with bending stiffness κ: Introducing $\Delta B(\kappa) \equiv B_{knot}(\kappa) - B_{linear}(\kappa)$, it follows that $\partial\Delta F_{knotting}(\kappa)/\partial\kappa = \Delta B(\kappa)$. The free energy cost of knotting is therefore

$$\Delta F_{knotting}(\kappa) = \Delta F_{knotting}(0) + \int_0^\kappa \Delta B(\kappa')\, d\kappa'$$

and thus

$$\Psi(\kappa) = \int_0^\kappa \Delta B(\kappa')\, d\kappa' \tag{4}$$

The existence of a minimum of $\Psi(\kappa)$ for $\kappa \neq 0$ will depend on the sign of the slope of $\Psi(\kappa)$ at $\kappa = 0$, $\Delta B(0)$. If $\Delta B(0) < 0$, we expect an optimal knotting rigidity $\kappa_{min} \neq 0$, whereas we anticipate a monotonically increasing function $\Psi(\kappa)$ in the opposite case, $\Delta B(0) \geq 0$. This is a reasonable expectation, since we will always obtain $\Delta B(\kappa) > 0$ for sufficiently stiff chains. Indeed, for $\beta\kappa \gg 1$, a linear polymer will adopt an almost straight configuration with $\hat{B} \approx 0$, as configurations with nonzero $\hat{B}$ are penalized by a high bending energy. $\hat{B} = 0$ is unique for the straight configuration, which is of course not
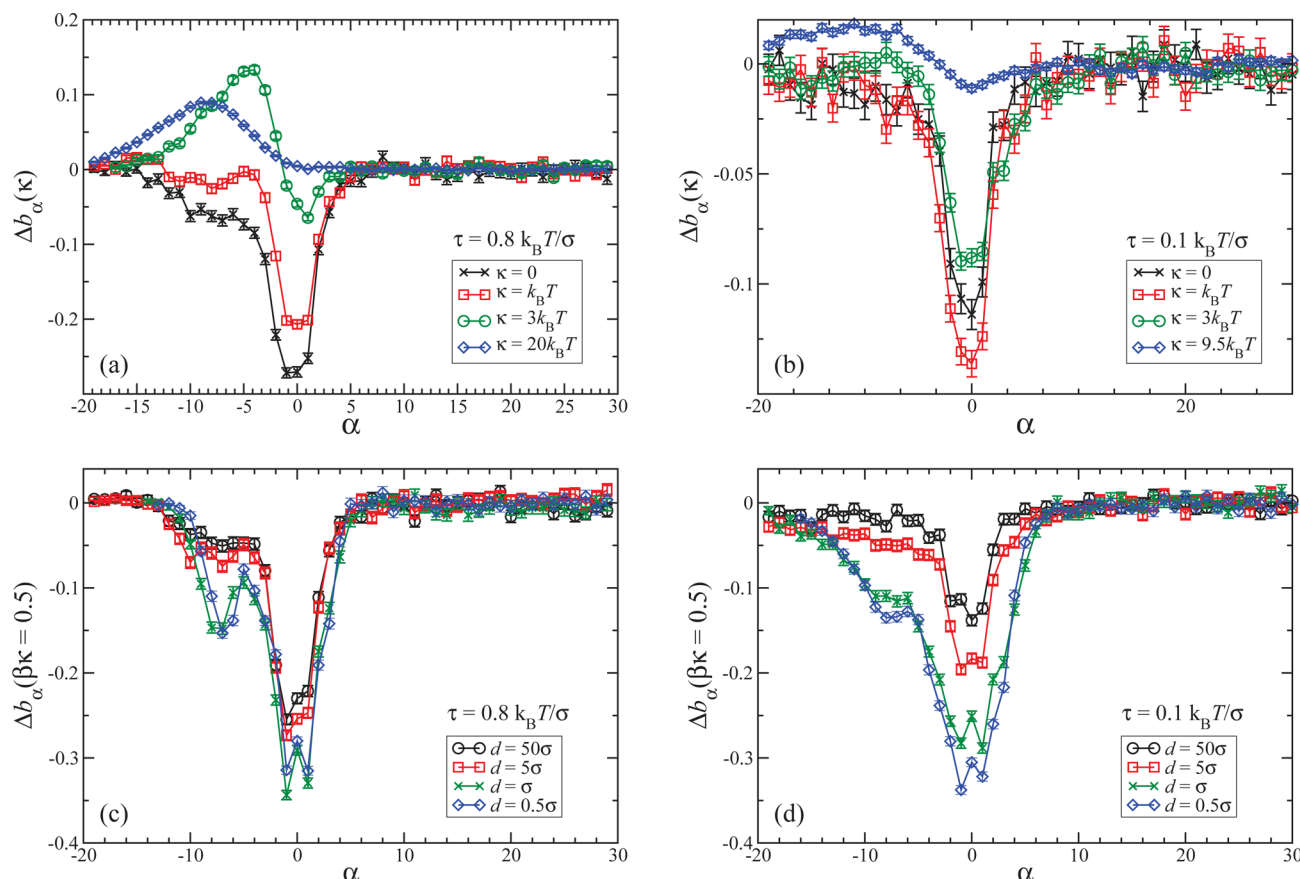
Figure 1. (a, b) Average local bending difference $\Delta b_\alpha(\kappa)$ (see text) between knotted and linear unconfined polymers of different rigidities, as indicated in the legend. (c, d) The same quantity at fixed bending rigidity $\kappa = 0.5\ k_B T$ for different degrees of slit confinement, as indicated in the legend. In panels a and c data for the tension $\tau = 0.8\ k_B T/\sigma$ are shown, while in panels b and d for $\tau = 0.1\ k_B T/\sigma$.

knotted. Therefore, $\Delta B(\kappa) > 0$ will hold for all knots in the $\beta\kappa \gg 1$ regime.

To illustrate this further, let us for example consider a stiff polymer chain with a trefoil knot. Its minimal energy is obtained for a straight polymer chain with an approximately circular domain at the location of the knot. The circle is tangent to the braid point and contains $N_K(\kappa) \cong [2\pi^2\kappa/(\tau l)]^{1/2}$ monomers, where $l \cong \sigma$ is the bond length.[21] Accordingly, $\Delta B(\kappa) \cong (2\pi^2\tau l)^{1/2}/\kappa > 0$ in this limit.

4. ANALYSIS OF THE LOCAL BENDING IN THE KNOTTED DOMAIN

Having in mind the goal of localizing which part of the polymer in the vicinity of the knot is contributing to an increased or decreased average bending and therefore to a nonvanishing $\Delta B(\kappa)$, we need to determine the knotted domain on the polymer chain. We define the knotted state of open subsections by introducing a topologically neutral closure scheme, which transforms an open string into a ring polymer that has a mathematically well-defined topological state.[22−24] We used a scheme where the end points of the open polymer are connected to a sphere at infinity in the direction of the vector from the centroid to the respective end point. The knotted part of the polymer chain is then the smallest domain for which the closure yields a ring polymer that has the correct Alexander polynomial.

Once the ends of the knot have been identified, we introduce a new enumeration scheme for the monomers, denoted by the Greek integer index α, which can have positive as well as negative values. The two monomers in the *interior* of the knot that lie n bonds away from the end points obtain the index $\alpha = -n$, whereas the two monomers to be found n bonds away at the *exterior* of the knot are assigned the index $\alpha = n$; accordingly, $\alpha = 0$ for the two end points of the knot. There exist, thus, for every value of α two position vectors $\mathbf{r}_\alpha^j$, $j = L, R$, where L/R denotes whether the monomer is at separation α from the left/right end point of the knot. Accordingly, we define the local bending contribution from the two monomers carrying the index α as

$$\hat{b}_\alpha \equiv \sum_{j=L,R} (1 - \hat{\mathbf{r}}_{\alpha-1,\alpha}^j \cdot \hat{\mathbf{r}}_{\alpha,\alpha+1}^j) \tag{5}$$

For $\alpha < 0$, $\hat{b}_\alpha$ measures the *local* bending of angles *in the interior* of the knot, while for $\alpha > 0$, $\hat{b}_\alpha$ measures the *local* bending *outside* of the domain that was identified as knotted. The domain limits for $\alpha \in [\alpha_{min}, \alpha_{max}]$ depend on the instantaneous configuration, as the number of monomers on the knot N_K determines how negative α can become. The range of α is constant, $\alpha_{max} - \alpha_{min} + 1 = N/2$.

We introduce a characteristic function $\hat{\chi}_\alpha = 1$ or 0 depending on whether the index α occurs for a given conformation or not and define the *local* bending difference between a knotted and a linear chain as

$$\Delta b_\alpha(\kappa) \equiv \langle \hat{\chi}_\alpha (\hat{b}_\alpha - b_{linear}(\kappa)) \rangle \tag{6}$$

In eq 6, $b_{\text{linear}}(\kappa) \equiv 2B_{\text{linear}}(\kappa)/N$ is the thermodynamic average of the bending of two angles on a linear chain. It follows that

$$\Delta B(\kappa) = \sum_{\alpha=-M}^{M} \Delta b_\alpha(\kappa) \tag{7}$$

where $M = N/2$ is the smallest value guaranteeing $[\alpha_{\min}, \alpha_{\max}] \subset [-M, M]$ for all polymer configurations.

5. RESULTS

Results for the local bending of unconfined polymers are shown in Figures 1a,b for two different values of the applied tension. As can be seen, the quantity $\Delta b_\alpha(\kappa)$ vanishes within less than 10 beads outside the knot; outside this region, a knotted chain hardly differs in its bending from an unknotted one. According to eqs 4 and 7, the area under the curves in Figures 1a,b determines the slope or $\Psi(\kappa)$ at any κ value. The major negative contribution to $\Delta B(\kappa)$ for $\kappa = 0$ comes from a small number of monomers close to the knot ends, i.e., in the braiding region of the knot, in which monomers start getting into the knotted domain. The bending suppression is therefore related to the interaction of the different strands at the crossings, which effectively confines the strands and hence reduces their random bending. Thus, the negative slope of $\Delta F_{\text{knotting}}(\kappa)$ at $\kappa = 0$ arises from this *additional* straightening of the knotted chain with respect to its flexible, unknotted counterpart. As $\Delta B(\kappa = 0)$, which is equal to the area under the respective curves in Figures 1a,b, is negative, a flexible knotted chain is, on average, *less bent* than its unknotted counterpart, contrary to the intuitive expectation that knotting inevitably *increases* the total bending of a polymer. In Figure 2 we show a
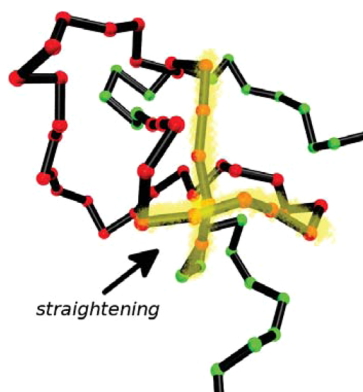

Figure 2. Simulation snapshot of the knotted domain of an unconfined, fully flexible polymer chain with a trefoil knot under the tension $\tau = 0.8\ k_B T/\sigma$. The straightened-out segments in the vicinity of the strand crossings are highlighted.

simulation snapshot of the knotted domain of a flexible chain, in which the parts of the molecule that get "straightened out" due to the knot are highlighted. As κ grows, we eventually reach the intuitively expected regime in which knotting increases bending; see, e.g., the curve for $\kappa = 20\ k_B T$ in Figure 1a, for which $\Delta B(\kappa) > 0$.

Comparing the curves of Figures 1a,b, one sees that $\Delta B(\kappa)$ for $\kappa = 0$ is more negative for $\tau = 0.8\ k_B T/\sigma$ than for $\tau = 0.1\ k_B T/\sigma$. This is due to the fact that at smaller τ the braid region is looser and the bending suppression due to the different strands at the crossings is reduced. On the contrary, if we increase κ, we arrive at a regime where $\Delta B(\kappa)$ is more negative

for smaller tensions τ. At $\beta\kappa = 3.0$, ΔB is already positive for $\tau = 0.8\ k_B T/\sigma$, due to the positive contribution of $\Delta b_\alpha(\kappa)$ in the interior of the knot, which arises as the knot enforces the polymer to form a loop. The bending throughout a loop is larger if the loop is smaller. For $\tau = 0.1\ k_B T/\sigma$ the knot size is increased, which is the reason why the positive $\Delta b_\alpha(\kappa)$ contribution in the interior of the knot is significantly smaller than for $\tau = 0.8\ k_B T/\sigma$. Accordingly, for lower tensions the negative net result for $\partial\Psi(\kappa)/\partial\kappa$ persists for higher κ-values than for higher tensions. As can be seen in Figure 1b, we see a reversal of $\partial\Psi(\kappa)/\partial\kappa$ from negative to positive values only at a rigidity as high as $\beta\kappa \cong 9$.

We now turn our attention to the confined case. It turns out that the effects of confinement are most transparent at a small, but nonzero, value of the bending rigidity; thus we show in Figures 1c,d results for $\Delta b_\alpha(\kappa)$ for $\beta\kappa = 0.5$, which is characteristic for all values of $\kappa \leq \kappa_{\min}$, the latter being the value of the rigidity for which $\Psi(\kappa)$ attains its minimum value $\Psi_{\min}$. Here, striking differences between the tensions $\tau = 0.8\ k_B T/\sigma$ and $\tau = 0.1\ k_B T/\sigma$ show up. While for $\tau = 0.8\ k_B T/\sigma$ there is hardly any difference between the confined and unconfined polymers for slit widths as small as $d = 5\sigma$, for $\tau = 0.1\ k_B T/\sigma$, confinement enhances Δb_α at the beginning of the knot by almost a factor 2. For both tensions, the suppression of bending through knotting becomes *even stronger* as a result of the geometric constraints, and thus $\Delta B(\kappa)$ is more negative for the polymer in the slit than it is for the free polymer. This is consistent with the interpretation given above for the case of the unconfined polymer, since the slit confinement forces the strands at the braid region to come closer which further reduces the random bending in the braid region. This effect, however, is more pronounced for smaller tensions, where the braiding region without confinement is looser than for polymer chains under higher tensions.

There exists a correlation between the slopes of $\Psi(\kappa)$ and $N_K(\kappa)$ shown in Figure 3. In the high-κ domain, $\Psi(\kappa) \sim N_K(\kappa) \sim \sqrt{\kappa}$, as is evident from the discussion following eq 4. For $\kappa = 0$, the knot is swollen due to the presence of steric interactions, maximizing in this way its entropy. However, for nonzero $\kappa \sim k_B T$, the fluctuations of the monomers are restricted in the first place, enabling thus a tighter braided region and a concomitant reduction of knot size. Thus, also for small κ the slopes of $\Psi(\kappa)$ and $N_K(\kappa)$ are expected to have the same sign. Note, however, that the value $\tilde{\kappa}$ that minimizes $N_K(\kappa)$ does not coincide with $\kappa_{\min}$, e.g., for very strong confinements $\kappa_{\min} \neq 0$, whereas $\tilde{\kappa}$ is, within simulation resolution, vanishingly small.

The dependence of the rigidity $\kappa_{\min}$ for which $\Psi(\kappa)$ has its minimum on the degree of confinement for different applied tensions is summarized in Figure 4a. We find that for a tension of $\tau\sigma = 0.8k_B T$ $\kappa_{\min}$ is only affected by confinement for slit widths lying at the monomer scale. In this regime of ultrastrong confinement, the energy cost that chain segments would have to pay to go one above the other in a gradual fashion at the braiding regions are too high. This is caused by the external potential, which assigns an increasingly high energetic cost for every monomer that deviates strongly from the $y = 0$-plane. Accordingly, it is preferable for the system to form localized "kinks" of one or two monomers in the braiding region, which expose a minimal number of monomers to the regions of high external potential, while at the same time creating strong bending there.

The situation is quite different, however, for lower tensions. In this case, also a moderate confinement of the order of 10
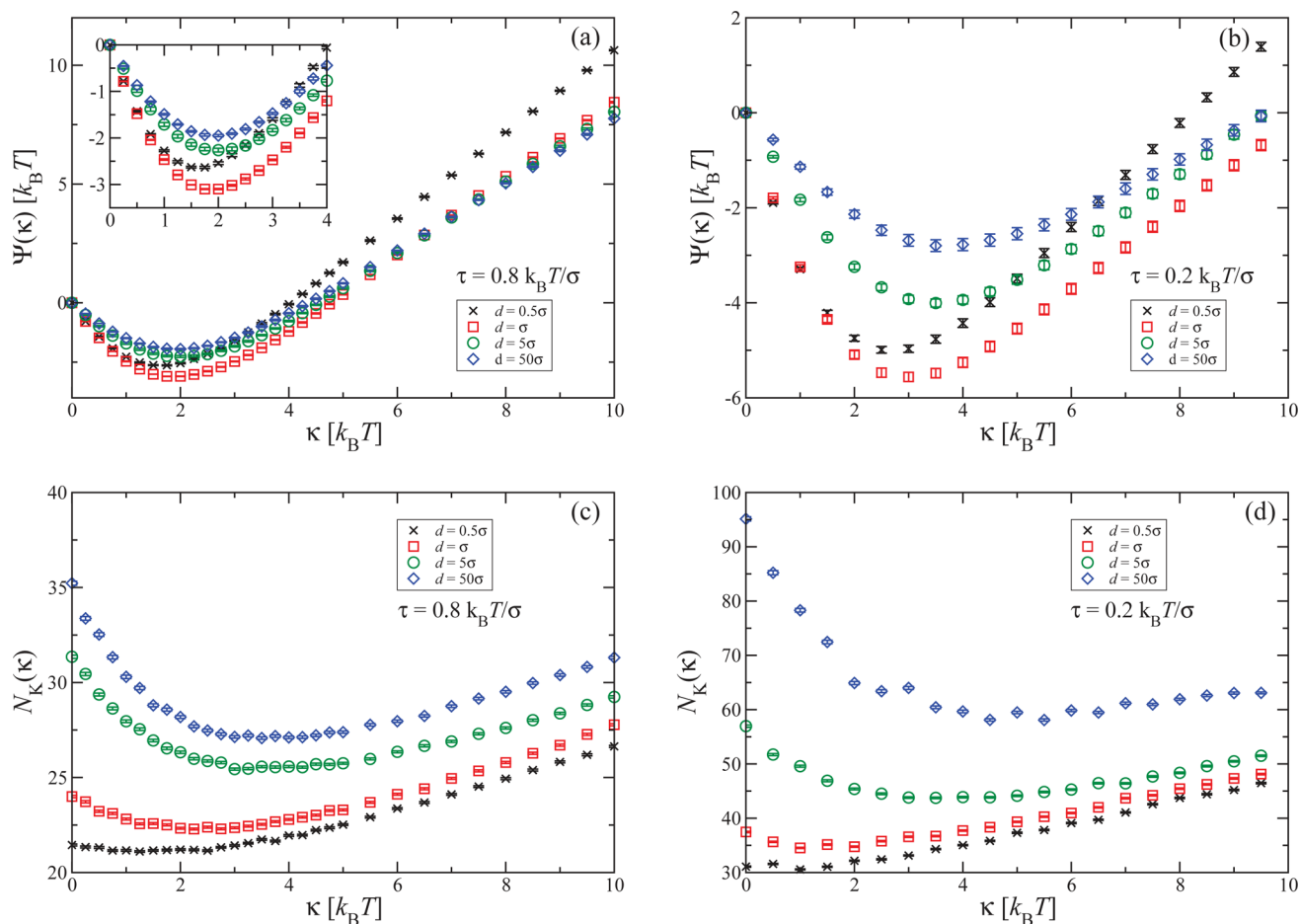
Figure 3. (a, b) The quantity $\Psi(\kappa)$ for different confinements, as indicated in the legend. The inset in (a) shows a zoom of the main panel in the region of the minimum of $\Psi(\kappa)$. (c, d) Dependence of the number of monomers in the knot, $N_K(\kappa)$, on chain rigidity. In panels a and c results for the tension $\tau = 0.8\ k_BT/\sigma$ are shown, whereas in panels b and d the tension is $\tau = 0.2\ k_BT/\sigma$.
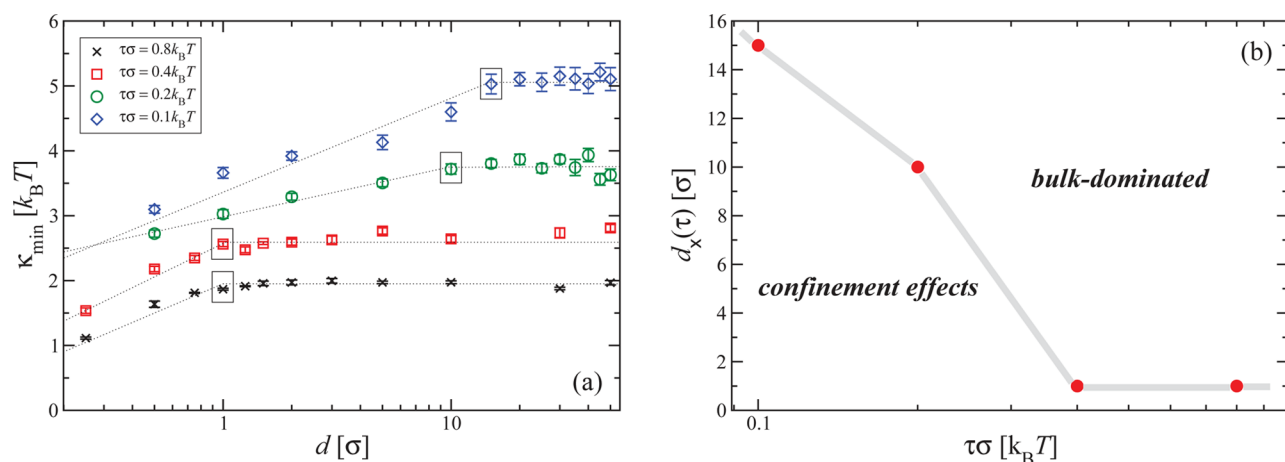

Figure 4. (a) Dependence of the optimal value for the rigidity, κ_{min}, on confinement for several applied tensions. The dotted lines are guides to the eye, delineating the two regimes where κ_{min} is influenced by confinement, where κ_{min} is d-dependent, and the bulk-dominated regime, where it is not. The crossover data points $d_\times(\tau)$ between the two regimes are marked with boxes. (b) Dependence of $d_\times(\tau)$ on the applied tension τ. The data points (red circles) are connected with thick gray segments, separating the bulk-dominated regime above the line by the confinement-affected regime below it.

bond lengths can significantly affect the value of κ_{min}. To better quantify the effects of confinement, we employ a simple, rough-and-ready separation of the data points shown in Figure 4a into two groups: for high values of d, the points form plateaus at the bulk values of κ_{min}, which we connect by horizontal lines.

Through the other groups of points straight lines are drawn by hand, which intersect the horizontal ones at tension-dependent crossover confinement widths $d_\times(\tau)$. These values denote, by construction, the crossover of the behavior of κ_{min} from bulk-dominated, for $d > d_\times(\tau)$, to confinement-affected, for $d <$
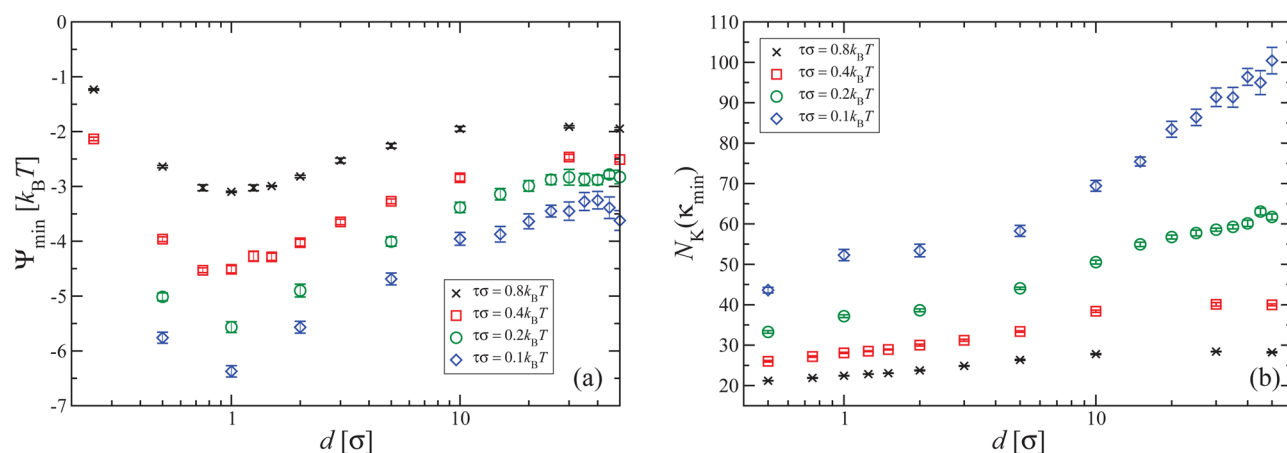
Figure 5. (a) Dependence of Ψ_{min}, the value of $\Psi(\kappa)$ at the optimal rigidity κ_{min}, on d, the slit-with of the confinement. (b) Knot size at the optimal rigidity as a function of d. Applied tensions as indicated in the legends.
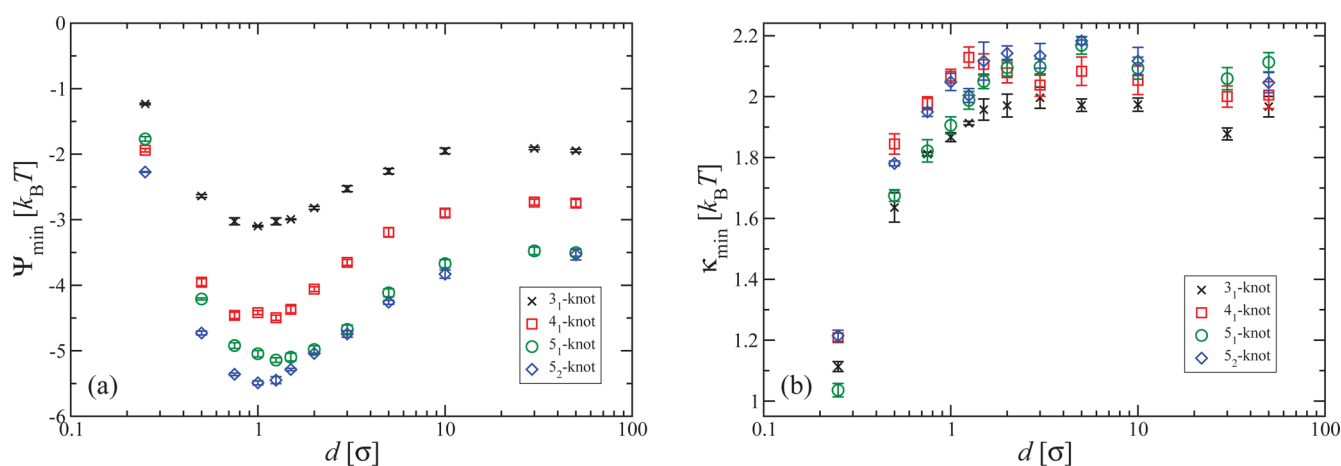

Figure 6. (a) Dependence of Ψ_{min} on confinement for tension $\tau = 0.8\ k_BT/\sigma$ and different knot types, as indicated in the legend. (b) The corresponding optimal value of the rigidity κ_{min} for different slit widths and knot types.

$d_\times(\tau)$. The results are summarized in Figure 4b, where it can be seen that $d_\times(\tau)$ is significantly increased for lower tensions. As we discuss below, the reason the situation is strikingly different for lower tensions seems to be related to the fact that the knot size is then significantly increased with respect to higher tensions.

The increased effects of confinement as τ decreases are also manifested on the value of Ψ_{min} as well as on the knot size $N_K(\kappa_{min})$. The former quantity is shown in Figure 5a and the latter in Figure 5b. As can be seen in Figure 5a, and in contrast to the values κ_{min} itself, even in the case of higher tension the corresponding depth of the minimum Ψ_{min} is influenced by a confining slit width of the order of 10 bond lengths. However, for lower tensions, the effect on Ψ_{min} is felt at even larger slit widths. Furthermore, the difference between the value Ψ_{min} in the bulk ($d/\sigma \gg 1$) and the one for the optimal slit width is enhanced. The fact that the effect of the confinement on the knot size is more pronounced for smaller tensions, as shown in Figure 5b, correlates well with the finding that confinement shifts κ_{min} to lower values for sufficiently small tensions. As we have seen in Figures 1a,b one of the contributions that eventually render $\partial\Psi(\kappa)/\partial\kappa$ positive is the bending in the interior of the knot, which arises as the knot enforces the polymer to form a loop. This contribution is larger for smaller knot sizes, and it is therefore consistent that κ_{min} will be shifted

by confinement if the latter is able to significantly reduce the knot size.

Up to now, all results have been derived for the simplest, trefoil knot; real polymers can, however, display a large variety of increasingly complex knots.[25,26] Considering other knots allows us on the one hand to put the general character of our results to the test and also to corroborate our assertion that the crossings at the braiding region are responsible for the reduction of $\Psi(\kappa)$ at finite κ-values. Indeed, more complex knots have more crossing points, where the strands of the polymer chain interact with each other. Thus, according to our analysis above, one should expect that a more complex knot will lead to lower values of $\Delta B(\kappa)$ and Ψ_{min} for small but finite κ. Our findings for different knot topologies (denoted in the Alexander–Briggs notation[27]) are summarized in Figures 6a,b. The data in Figure 6a confirm that the main effect of the increased knot complexity is the addition of crossing points which all result in a similar bending suppression as the crossing points of the trefoil knot. Accordingly, for the knot topologies investigated, Ψ_{min} is approximately proportional to the number of minimal crossings of the respective knot diagram, at least for confinements with $d \geq \sigma$. It is also striking that for the unconfined case Ψ_{min} is, within error bars, identical for the 5_1 and 5_2 topologies. A test of whether Ψ_{min} is in good approximation proportional to the minimal number of

crossings of arbitrarily complex knots is beyond the scope of this work. However, the number of strand crossings will increase with knot complexity. Accordingly, the free energy penalty for putting a knot on a stiff polymer ($\kappa \neq 0$) can be much lower than the one for putting it on a fully flexible polymer ($\kappa = 0$), by amounts that grow with the knot complexity. Whereas Ψ_{min} is sensitive to the knot type, κ_{min} is not, as can be ascertained from the results shown in Figure 6b. All data fall within a narrow band of width $\Delta\kappa_{min} \cong 0.2k_BT$ irrespective of the knot topology.

The tensions considered in our work are of the order of k_BT/σ. At room temperature and a monomer length scale of 1 nm this corresponds to the pN scale. These tensions result in values of $\kappa_{min} \approx 5\ k_BT$. As it was found in previous work,[1] without confinement κ_{min} scales approximately as $\sim\tau^{-1/2}$. A reduction of the tension down to the fN scale, which is typical of double-stranded DNA molecules,[28] will bring κ_{min} at the order of 100 k_BT. Our results imply that at these lower tensions the effect of confinement on κ_{min} can be expected to be even more pronounced.

6. CONCLUSIONS

In summary, we have demonstrated that the local stretching at the braiding region and close to the crossing points is the physical mechanism responsible for the minimization of the free energy penalty of knotting of a linear polymer for nonvanishing values of the bending rigidity. Confinement can affect the location of the optimal rigidity for sufficiently low tensions, when it is at the same time significantly affecting the knot size. We therefore expect the geometrical reduction of dimensionality to become relevant for the location of the knots of chains with variable rigidity if the latter are under sufficiently small tensions. For tensions at the fN scale, which are typical of double-stranded DNA molecules,[28] we therefore expect that confinement to strongly influence the value of the optimal rigidity. On the other hand, the amount of reduction of the knotting of free energy by rigidity strongly depends on the topology of the knot, and it increases with the knot complexity, scaling roughly with the number of minimal crossings of the knot. Accordingly, we anticipate that more complex knots will localize more strongly in the optimal regions of a chain than simpler ones. Recent advances in tying knots on polymers by optical tweezers[29,30] and adsorbing them on mica surfaces[15] should allow for experimental testing of our predictions.

■ AUTHOR INFORMATION

Corresponding Author

*E-mail: peter.poier@univie.ac.at (P.P.).

Notes

The authors declare no competing financial interest.

■ REFERENCES

(1) Matthews, R.; Louis, A. A.; Likos, C. N. *ACS Macro Lett.* **2012**, *1*, 1352.

(2) Sogo, J. M.; Stasiak, A.; Martínobles, M. L.; Krimer, D. B.; Hernández, P.; Schvartzman, J. B. *J. Mol. Biol.* **1999**, *286*, 637.

(3) Arsuaga, J.; Vázquez, M.; Trigueros, S.; Sumners, D. W.; Roca, J. *Proc. Natl. Acad. Sci. U. S. A.* **2002**, *99*, 5373.

(4) Portugal, J.; Rodrguez-Campos, A. *Nucleic Acids Res.* **1996**, *24*, 4890.

(5) Deibler, R. W.; Mann, J. K.; Sumners, De Witt L.; Zechiedrich, L. *BMC Mol. Biol.* **2007**, *8*, 44.

(6) Liu, Z.; Deibler, R. W.; Chan, H. S.; Zechiedrich, L. *Nucleic Acids Res.* **2009**, *37*, 661.

(7) Hogan, M.; LeGrange, J.; Austin, B. *Nature* **1983**, *304*, 752.

(8) Geggier, S.; Vologodskii, A. *Proc. Natl. Acad. Sci. U. S. A.* **2010**, *107*, 15421.

(9) Johnson, S.; Chen, Y.-J.; Phillips, R. *PLoS One* **2013**, *8*, e75799.

(10) Rybenkov, V. V. *Science* **1997**, *277*, 690.

(11) Emanuel, M.; Hamedani Radja, N.; Henriksson, A.; Schiessel, H. *Phys. Biol.* **2009**, *6*, 025008.

(12) Jun, S.; Mulder, B. *Proc. Natl. Acad. Sci. U. S. A.* **2006**, *103*, 12388.

(13) Purohit, P. K.; Inamdar, M. M.; Grayson, P. D.; Squires, T. M.; Kondev, J.; Phillips, R. *Biophys. J.* **2005**, *88*, 851.

(14) Orlandini, E.; Stella, A. L.; Vanderzande, C. *Phys. Biol.* **2009**, *6*, 025012.

(15) Ercolini, E.; Valle, F.; Adamcik, J.; Witz, G.; Metzler, R.; de los Rios, P.; Roca, J.; Dietler, G. *Phys. Rev. Lett.* **2007**, *98*, 058102.

(16) Micheletti, C.; Orlandini, E. *Macromolecules* **2012**, *45*, 2113.

(17) Matthews, R.; Louis, A. A.; Yeomans, J. M. *Mol. Phys.* **2011**, *109*, 1289.

(18) Plimpton, S. *J. Comput. Phys.* **1995**, *117*, 1.

(19) Tuckerman, M. E.; Liu, Y.; Ciccotti, G.; Martyna, G. J. *J. Chem. Phys.* **2001**, *115*, 1678.

(20) Rubinstein, M.; Colby, R. *Polymer Physics*; Oxford University Press: Oxford, 2003.

(21) Gallotti, R.; Pierre-Louis, O. *Phys. Rev. E* **2007**, *75*, 031801.

(22) Tubiana, L.; Orlandini, E.; Micheletti, C. *Prog. Theor. Phys. Suppl.* **2011**, *191*, 192.

(23) Marcone, B.; Orlandini, E.; Stella, A. L.; Zonta, F. *Phys. Rev. E* **2007**, *75*, 041105.

(24) Marcone, B.; Orlandini, E.; Stella, A. L.; Zonta, F. *J. Phys. A: Math. Gen.* **2005**, *38*, L15.

(25) Koniaris, K.; Muthukumar, M. *Phys. Rev. Lett.* **1991**, *66*, 2211.

(26) Rawdon, E.; Dobay, A.; Kern, J. C.; Millett, K. C.; Piatek, M.; Plunkett, P.; Stasiak, A. *Macromolecules* **2008**, *41*, 4444.

(27) Livingston, C. *Knot Theory*; Carus Monographs; Mathematical Association of America: Washington, DC, 1993; Vol. 24.

(28) Gutjahr, P.; Lipowsky, R.; Kierfeld, J. *Europhys. Lett.* **2006**, *76*, 994.

(29) Arai, Y.; Yasuda, R.; Akashi, K.; Harada, Y.; Miyata, H.; Kinoshita, K., Jr.; Itoh, H. *Nature* **1999**, *399*, 446.

(30) Bao, X. R.; Lee, H. J.; Quake, S. R. *Phys. Rev. Lett.* **2003**, *91*, 265506.